SIMULATION OF BOGIE DYNAMICS UNDER HEAVY BRAKING

Yunendar Handoko and Manicka Dhanasekar

Centre for Railway Engineering

Central Queensland University

Rockhampton 4702, Australia.

SUMMARY

The importance of including the events of braking / traction to the simulation of wagon dynamics is increasingly recognised due to damages caused to running surfaces by these events. To realistically include these events, explicit definition of wheelset pitch degree of freedom in the formulation of the system equation is necessary. This paper presents such a formulation and demonstrates its effectiveness in predicting wheel skid due to heavy braking when the braking force exceeds the adhesion available at the wheel-rail interface. A model of single wheelset bogie and a bogie model containing two wheelsets within a rigid bogie frame are used as illustrative examples. It is shown that the bogie dynamics is affected differently due to sudden heavy braking either at the leading wheelset alone or at both wheelsets simultaneously.

1. INTRODUCTION

Heavy braking severely affects the dynamics of bogies and hence that of wagons; this situation could lead to disastrous effects such as wheel skid and derailment. Therefore, field or lab testing of the event is generally avoided and an understanding could only be developed using computer simulation which in itself is a complex task as the speed no longer remains constant under braking. Current wagon dynamics software packages (for example, VAMPIRE [1]) primarily deal with constant speed simulations only; the effect of braking is simulated by pre-defining a speed profile. This limitation is due to the adoption of a track following reference frame which moves at pre-defined speed as the modelling platform. However, the speed profile of vehicles is affected by a large number of parameters during braking. Thus, it is not easy to define a speed profile corresponding to an event of brake application as a priori. An appropriate approach would be to input the braking force into the simulation model and allow the model to calculate the speed profile of the wagon. For this purpose, wheelset pitch should be included in the modelling.

A special purpose program has therefore been developed by the first author, which accounts for the wheelset pitch as a degree of freedom explicitly with the capability of defining braking (or traction) torques directly to the wheelsets. The program couples the longitudinal and the lateral dynamics as a natural process. For this purpose, the equation of motion is defined in the fixed reference frame platform. With this method of modelling it would be possible to thoroughly investigate the dynamic characteristics of wagons during braking or traction where the speed and wheelset pitch no longer remain constant.

2. WAGON BRAKING SYSTEM

Braking may be regarded as a process of energy conversion. A moving rail wagon possesses significant kinetic energy. Reducing the speed of the wagon requires significant reduction to the kinetic energy. The simplest way of reducing the energy is to convert it into heat through contacting material to the rotating wheels or to discs attached to the axles. The contact creates friction and converts the kinetic energy into heat energy. With the reduction in kinetic energy, the wagon slows down and when the kinetic energy is fully exhausted, the wagon comes to static equilibrium.

The vast majority of wagons, especially freight wagons, are equipped with braking systems which use compressed air to generate the required force to push blocks onto wheels. These systems are known as pneumatic brakes. In this system the compressed air is transmitted along the train through pipes. A valve controls the pressure level of the compressed air used to produce the braking force.

The braking force produced by the brake cylinder is transmitted through a set of levers and rods to the bogie. The force is then distributed to the wheels through the brake rigging, which consist of levers and brake beams linked with pins and bushes, fitted in each bogie. Fig.1 shows a typical diagram of the brake rigging arrangement of the three-piece bogie which is widely used in freight wagons [2].

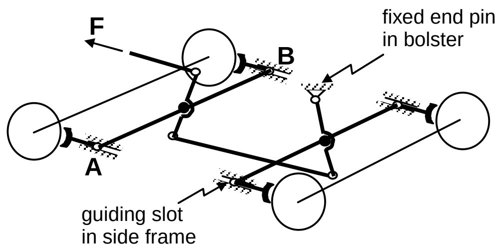

Fig.1. Brake rigging arrangement [4]

3. FORCES ON A WHEEL DUE TO BRAKING

3.1. Basic Principle

Application of braking generates forces or torques to the wheels which subsequently reduces their speed. This process also produces reaction forces in couplers and pitch torque to the wagon body and bogie. These forces can affect the running stability and curving performance of wagons.

On the other hand the change of the load distribution to wheels also affects the braking performance. The braking performance is usually measured through the stopping distance and also from skidding or wheel slide. With the reduction of the wheel load, the chance of skid occurrence increases.

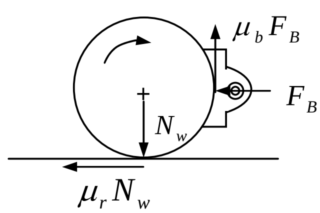

Fig.2. Force effective at the braked wheel

Braking involves friction, a subject that has attracted many researchers for decades due to its complexity. Frictional phenomena are complex in nature as no simple laws can be supposed to be rigorously true under all conditions. During the process of braking, friction develops between brake shoe and wheel as well as between wheel and rail. The brake shoe force applied to the wheel F_B produces tangential force $\mu_b F_B$ (see Fig.2), where μ_b is the friction coefficient between the shoe and the wheel. If the wheel radius is r_0, a braking torque T_B is generated as defined below.

$$T_B = \mu_b F_B r_0 \quad (1)$$

T_B acting on the wheel brings it to rest.

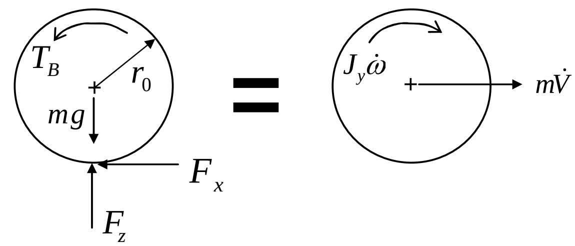

Fig.3. Free body diagram of braked wheel

Consider a wheel shown in Fig.3 that moves longitudinally in the x-direction at speed V and with angular velocity ω. J_y, r_0 and T_B denote the polar moment of inertia, wheel radius and brake torque respectively. At the contact point between wheel and rail a longitudinal force F_x and vertical force F_z arise as a reaction to the brake torque and the static load mg. By balancing the forces in the x- and z- directions and moments about the centre of mass of the wheel, we obtain the following three basic scalar equations for a braked wheel system:

$$\begin{aligned} m\dot{V} &= -F_x \\ F_z &= mg \\ J_y\dot{\omega} &= F_x r_0 - T_B \end{aligned} \quad (2)$$

where m is the mass of the wheel and wagon supported by the wheel and g is the acceleration due to gravity; over dots denote differentiation with respect to time.

3.2. Skidding and Friction Coefficient

Severe braking force can lock the wheelset and contributes to its skidding on the rail. Skidding leads to geometry damage (flat) to the wheel and to the railhead. Skidding also makes the stopping distance longer. Hence skidding should be avoided during braking as a matter of priority.

Skidding occurs when the braking force exceeds the adhesion offered by the wheel-rail contact patch. Thus, to avoid skidding of the wheels during brake application the brake force at the brake shoe must be invariably kept lower than the adhesion at the rail. Skidding will not occur when the relationship in Eq.(3) is fulfilled.

$$\mu_b F_B < \mu_r N_W \tag{3}$$

where μ_b is friction coefficient between the wheel and the shoe, μ_r is friction coefficient between the wheel and the rail, F_B and N_w are brake force and normal load at wheel-rail contact point respectively.

Currently many rail wagons, especially passenger cars, are equipped with expensive equipment to prevent skid. However, many freight wagons do not possess such equipment.

The difficulty of controlling the skidding is associated with friction characteristics between the wheel and the rail which varies with rail surface condition [3]. The surface condition that could affect the friction characteristic includes rail corrugations, rail head contamination such as oily deposits, leaves, water, ice, sand, etc. The wheel tread surface condition due to the application of the different type of brake shoe on the car (iron block, composition block, disc) can also affect the friction characteristics. Friction between wheel and rail also varies with the position of the wheelset along the track. The leading wheelset usually encounters the dirtiest rail and hence the worst adhesion condition relative to the other wheels. In spite of these uncertainties, for design purpose the friction coefficient between wheel and rail is usually assumed between 0.1 - 0.3.

4. FORMULATION OF MULTIBODY DYNAMICS SYSTEM

4.1. Equation of Motion

The equation of motion of a multibody system that involves contact constraints between the wheel and the rail can be written in an augmented form that contains generalised coordinates and non-generalised surface parameters as shown in [4] :

$$\begin{bmatrix} \mathbf{M} & \mathbf{0} & \mathbf{C}_\mathbf{q}^\mathrm{T} \\ \mathbf{0} & \mathbf{0} & \mathbf{C}_\mathbf{s}^\mathrm{T} \\ \mathbf{C}_\mathbf{q} & \mathbf{C}_\mathbf{s} & \mathbf{0} \end{bmatrix} \begin{bmatrix} \ddot{\mathbf{q}} \\ \ddot{\mathbf{s}} \\ \boldsymbol{\lambda} \end{bmatrix} = \begin{bmatrix} \mathbf{Q} \\ \mathbf{0} \\ \mathbf{Q}_d \end{bmatrix} \tag{4}$$

where $\mathbf{M}$ is the mass matrix, $\mathbf{C}_\mathbf{q}$ and $\mathbf{C}_\mathbf{s}$ are constraint Jacobian matrices in respect to generalised coordinates $\mathbf{q}$ and surface parameter $\mathbf{s}$ respectively, $\boldsymbol{\lambda}$ is the vector of Lagrange multiplier, $\mathbf{Q}_d$ is a vector that absorbs quadratic terms in the first time-derivatives of the generalised coordinates and the surface parameters, and $\mathbf{Q}$ is the sum of the vectors of generalised applied force $\mathbf{Q}_e$ and the quadratic velocity vector $\mathbf{Q}_v$ as shown in Eq. (5).

$$\mathbf{Q} = \mathbf{Q}_e + \mathbf{Q}_v \tag{5}$$

For the body i the quadratic velocity vector $\mathbf{Q}_v$ is given in reference [6] as follow:

$$\mathbf{Q}_v = \begin{bmatrix} \mathbf{0}^\mathrm{T} & -2\bar{\boldsymbol{\omega}}^{i\mathrm{T}} \mathbf{I}_{\theta\theta}^i \dot{\bar{\mathbf{G}}}^i \end{bmatrix} \tag{6}$$

where $\bar{\boldsymbol{\omega}}^i$ is the angular velocity vector defined in the body coordinate system, $\mathbf{I}_{\theta\theta}^i$ is the inertia tensor, $\bar{\mathbf{G}}^i$ is the matrix that relates the angular velocity vector to the time derivatives of the orientation coordinates, and superscript T denotes the matrix transpose. The vector of the generalised applied force $\mathbf{Q}_e$ includes externally applied forces such as braking or traction forces, gravity forces, suspension forces and creep forces, excluding the constraint forces which are automatically eliminated using the virtual work principle. In the case of wheel-rail contact, the constraint forces are the normal forces that work on the contact patch which are calculated using the vector of Lagrange multiplier $\boldsymbol{\lambda}$.

4.2. Modelling the Wheel and the Rail Surfaces

The first step in detecting the points of contact accurately is to describe the location of all points on the surfaces of the wheel and the rail in space. This becomes difficult as the wheel and the rail surface profiles are usually complex and cannot be defined by a simple analytical expression. However in general, the surface profiles of the wheel and the rail can be seen as being generated from two-dimensional curves [4] as shown in Figs. 4 and 5 (for new wheels and rails with no localised damage) respectively.

Wheels are described as a surface obtained by rotating a two-dimensional curve (Eq. 7) that defines the wheel profile through 360 degrees about the wheel axis as shown in Fig. 4.

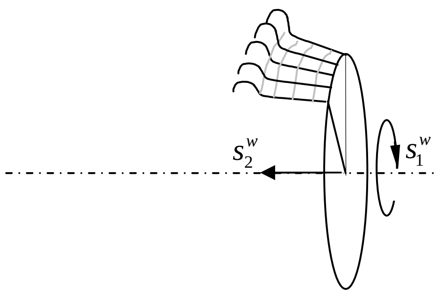

Fig.4. Wheel surface profile

Coordinate of any point on the wheel surface can be defined mathematically as follows:

$$\left.\begin{aligned} x &= x_0 + r(s_2^w)\sin s_1^w \\ y &= y_0 + s_2^w \\ z &= z_0 - r(s_2^w)\cos s_1^w \end{aligned}\right\} \qquad (7)$$

where s_1^w and s_2^w are the surface parameters of the wheel. In this case the parameter s_1^w represents the rotation about the wheel axis and the parameter s_2^w represents the translation in the lateral direction.

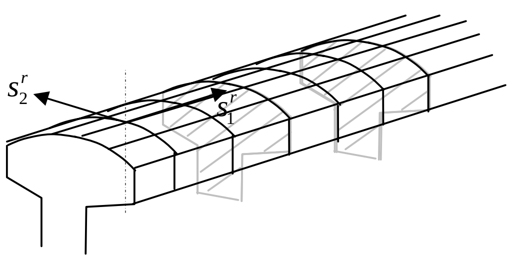

Fig.5. Rail surface profile

Rail is described by translating a two-dimensional curve that defines the rail profile (Eq. 8) in the longitudinal direction as shown in Fig. 5. Coordinate of any point on the rail surface can be defined as

$$\left.\begin{aligned} x &= x_0 + s_1^r \\ y &= y_0 + s_2^r \\ z &= z_0 + f(s_2^r) \end{aligned}\right\} \qquad (8)$$

where s_1^r and s_2^r are the surface parameters of the rail. The parameter s_1^r represents the longitudinal translation and the parameter s_2^r represents the lateral translation.

4.3. Solution Technique

Eq.(4), which is a mixed set of differential and algebraic equations, is solved by using the coordinate partitioning method. The dependent and independent coordinates are partitioned and selected by using Gauss elimination. By providing a set of initial conditions, the independent coordinates are integrated forward in time using the Runge-Kutta method [5]. The output of the solution process defines the independent coordinates and velocities as well as the independent surface parameters and their first derivatives. From these quantities the dependent coordinates and surface parameters are determined from the nonlinear kinematic relation of the constraint equations by using iterative procedure of Newton-Raphson algorithm.

5. SIMULATION RESULTS

5.1. Single Wheelset Bogie

In order to understand the railway wagon dynamics, it is common to investigate the motion of a single wheelset running on the tangent track. Therefore, in this investigation a wheelset connected to a mass by a set of linear springs and dampers in the longitudinal, the lateral, and the vertical directions as shown in Fig.6, was considered. The characteristics of the springs and dampers are presented in Table 1, the values of which were selected in such a way that the critical speed (the speed where the wheelset motion becomes unstable) was around 100 km/h (27.7 m/s). As a reference, the critical speed of wagons containing three-piece bogies running on the rigid track calculated by Sun and Dhanasekar [6] is in the range between 79 km/h – 159 km/h, depending on the wheel profile used.

Table 1 Spring and damper characteristics

	Spring Stiffness , K (N/m)	Damping Coefficient, C (N.s/m)
Longitudinal	20×10^4	10×10^3
Lateral	8×10^4	6×10^3
Vertical	5×10^4	4×10^3

The inertia properties of the wheelset and the bogie frame used in the simulation are given in Table 2. The mass and mass moment of inertia of the unsprung mass were chosen so that the axle load reflects the common normal operation of four axle wagons. The friction coefficient between the wheel and the rail was set constant at 0.3.

Table 2. Inertia properties of the wheelset and the Sprung Mass

Components → / Properties↓	Wheelset	Sprung Mass
M (kg)	1200	10000
I_{xx} ($\mathrm{kg \cdot m^2}$)	720	20000
I_{yy} ($\mathrm{kg \cdot m^2}$)	112	15000
I_{zz} ($\mathrm{kg \cdot m^2}$)	720	20000

As the bogie frame is supported only by two vertical springs (on the left and the right), an unbalanced moment with respect to the lateral axis will act on the bogie frame. In anticipation of this, a constraint was added to eliminate the pitch degree of freedom of the bogie frame. Thus the bogie frame was represented with five degrees of freedom. The springs and dampers were attached to the wheelset at the points on the axis of rotation of the axle (lateral axis of wheelset body reference frame). By using such arrangement the points of connection did not rotate about the axle so the additional revolute joint is not needed.

For generalisation, the left and the right rails were considered as separate bodies constrained to the ground. Thus, the total number of bodies in the system was four (the right rail, the left rail, wheelset and bogie frame). With this assumption it was possible to simulate different lateral and vertical irregularities for each rail and also track gauge widening at the curve where the outer and inner rail each had a different curve radius. In spite of these opportunities, this paper has neither considered the rail geometry irregularity nor other defects due to its primary focus on the effect of longitudinal forces to wheelset dynamics.

First a simulation was performed at a constant speed of 25 m/s. At a specified distance of travel a lateral disturbance in the form of track lateral displacement was provided to the wheelset to initiate lateral oscillation. Fig.7. shows the wheelset and the bogie frame lateral displacement against the travel distance. The figure also shows that the system remains stable which is shown by the damped lateral oscillation. The oscillations have had a 13.25 m wavelength; or, for a speed of 25 m/s, a frequency of 1.89 Hz.

a. Top view

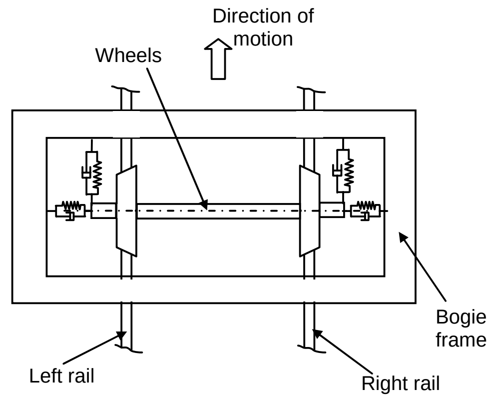

b. Front view

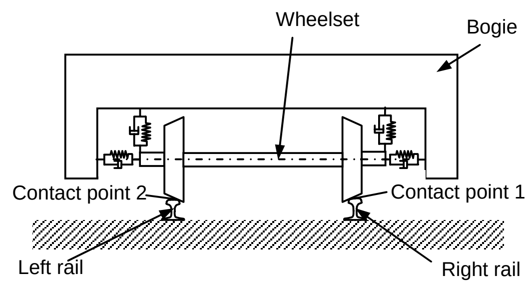

Fig.6. Single wheelset bogie

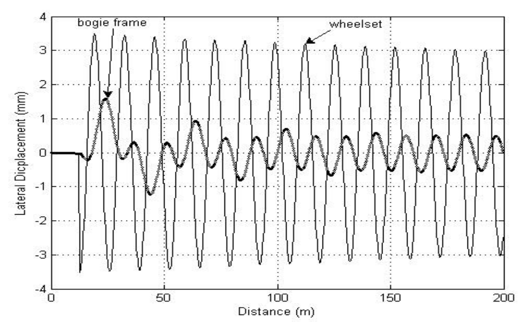

Fig.7. Wheelset lateral displacement V=25 m/s

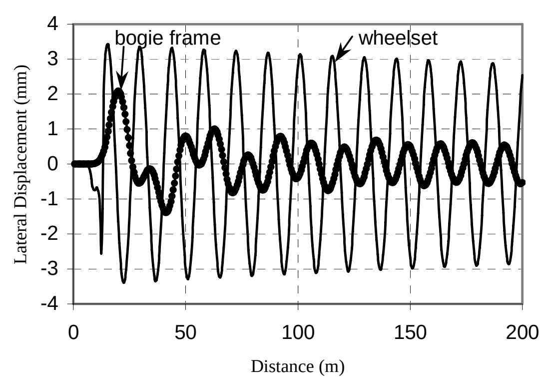

Fig.8. Lateral displacements calculated by VAMPIRE at V=25m/s

A simulation of equivalent system at 25 m/s is also performed by using VAMPIRE. The VAMPIRE result is shows in Fig.8 which agrees well with the previous result provided by the current computer program.

To simulate the effects of heavy braking, a large brake torque (25kN.m) was then applied to the wheelset. With a friction coefficient of 0.3 and the total mass of the system of 11200 kg, the maximum longitudinal force that could be generated was approximately 16.48kN at each rail. At the nominal wheel radius of 0.425m, the associated brake torque that could cause the wheelset to be braked without slip was around 14kN.m only.

The heavy brake simulation at an initial speed of 25m/s is shown in Fig.9. Brake torque was applied at t = 2.5 sec. From Fig.9 (b) it can be seen that the wheelset rotation has quickly decreased to zero in about 1 sec while the speed was still more than 20m/s. This means that the wheel stopped rotating while it was still moving forward (skid). Fig.9(c) shows the lateral displacement of the wheelset. The figure shows very clearly that at the time of skid initiation, the motion of the wheelset became unstable with very low frequency of oscillation.

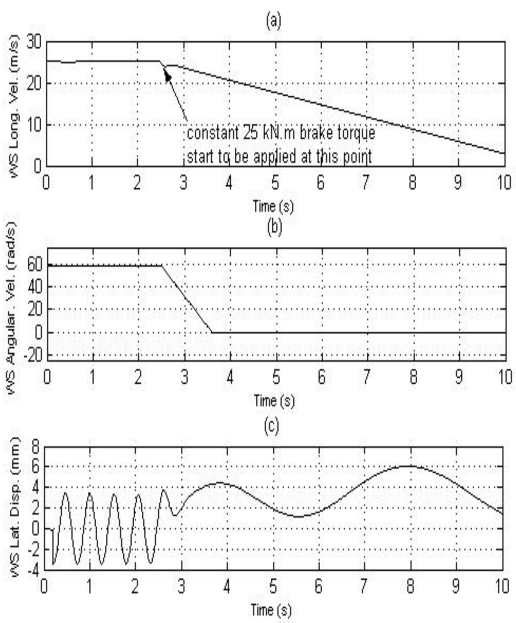

Fig.9. Skid of single wheelset bogie

5.2. Two Wheelsets Bogie

The previous problem was extended to a problem of one simple bogie with two wheelsets. The top view of the bogie is presented in Fig.10. The bogie system parameters such as mass, moment inertia and spring and damper characteristics refer to the vehicle model presented in Section 6.5 in [7].

First the simulation was conducted at the constant speed of 20 m/s to examine the stability of the system. It was found that at this speed the bogie was still stable as evidenced by the sustained small level of the lateral oscillation shown in Fig.11.

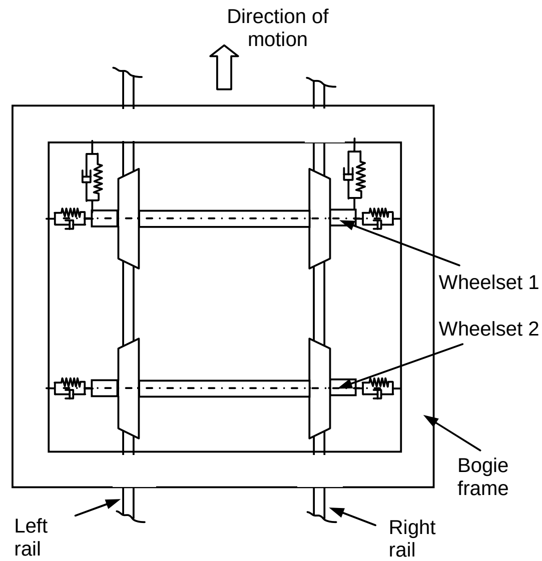

Fig.10. Top view of two-wheelset bogie

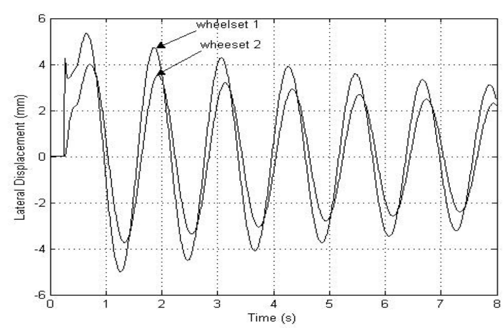

Fig.11.Wheelset lateral displacement at V = 20m/s

Then two cases of braking were studied. The first case concerned applying a large brake torque to the leading wheelset while the trailing wheelset was left unbraked. The initial speed was V=20 m/s. This condition caused skidding of the leading wheelset as shown in Fig.12. This figure shows that the angular velocity of the leading wheelset has decreased rapidly to zero (Fig.12 (b)) while the forward speed and the angular velocity of the trailing wheelset remains much greater than zero (Fig.12 (a) and (c)). Just before the application of braking, a lateral force was applied on the first wheel to initiate lateral oscillation. The related lateral displacement is presented in Fig.13. It was found that the skidding wheelset remained unstable resulting in flange contact. While the leading wheelset had an excessive lateral displacement, the unbraked trailing wheel remained stable and there was an indication that it could help stabilize the leading wheelset oscillation as shown by the slight reduction of the leading wheelset oscillation at the end of simulation. However, this situation could have also resulted from the effect of the reducing speed.

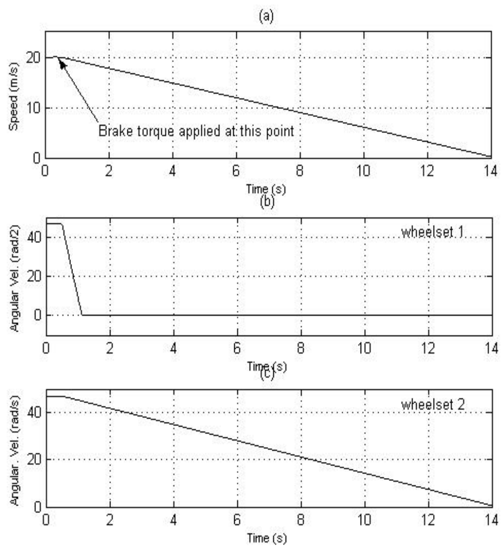

Fig.12. Skid on one wheelset

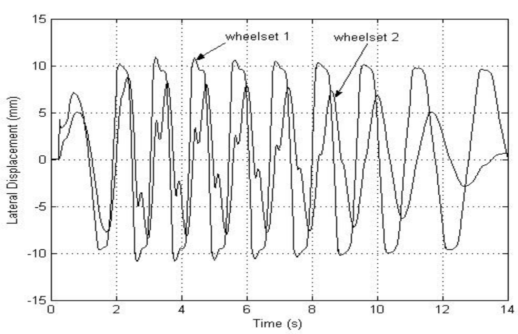

Fig.13. Lateral displacement; skid on one wheeslet

The second case of braking was the same large braking torques applied to both wheesets. As predicted it caused skidding of both wheelsets as shown in Fig.14. This figure shows the angular velocity of both wheelsets rapidly decreases to zero while the speed remains much greater than zero. Similar to the previous simulation, an impulse force had been applied to the leading wheelset just before the braking was applied to initiate the lateral oscillation. The lateral displacement time history is shown in Fig 15. The figure shows a very low frequency oscillation which is unstable at the beginning and then sustained due to very low speed.

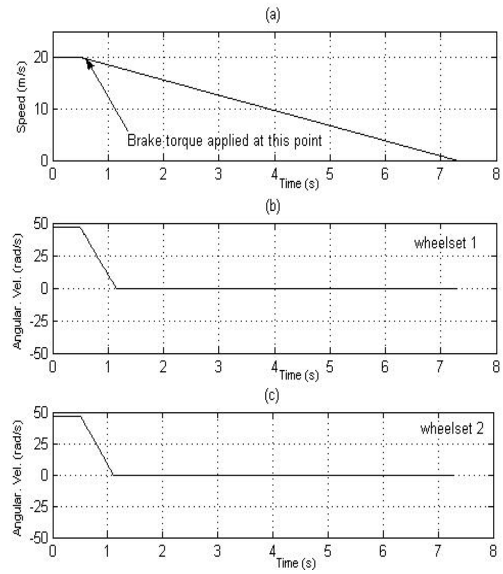

Fig.14. Skid on two wheelsets

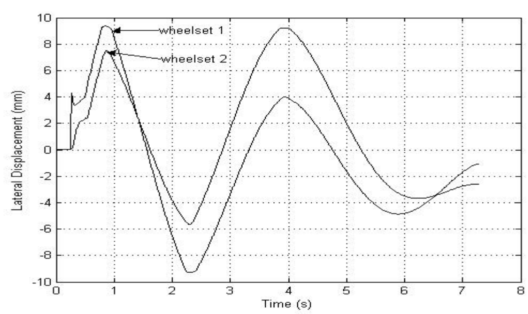

Fig.15. Wheelset lateral displacement; skid on two wheelset

6. CONCLUSION

Braking and traction induces severe dynamics to the running wheelsets and bogies (and to wagons). Unfortunately most commercially available wagon dynamics software package do not account for braking/traction; these effects are implicitly accounted for by speed profile as a priori. As the speed profile is affected by a number of parameters including the non-linear contact parameters, it is not always possible to define speed profile as a function of braking/traction. This paper therefore has described a method of explicitly accounting for braking/traction issues by including the wheelset pitch degree of freedom. This necessitates adoption of a fixed coordinate reference system and formulation of mixed set of differential and nonlinear algebraic equations central to the mathematical model. By solving this set of equations numerically, the effect of brake force application to the wheelset pitch and running speed has been determined. From this research the following conclusions are made:

1. It is necessary to include the wheelset pitch degree of freedom explicitly in the multibody system dynamics equations to effectively account for the effect of braking/traction application to the dynamics of wheelsets, bogies and wagons.
2. The computer program developed as part of this research (i.e, by including wheelset pitch dof) produces results comparable to that of VAMPIRE for constant speed simulation cases - thus validating the program / model / solution techniques considered.
3. When sudden heavy braking is applied to one wheelset of a bogie running at constant initial speed, the braked wheelset's rotation comes to rest quickly while the whole bogie system still has forward velocity leading to skidding and instability of the braked wheelset.
4. When sudden heavy braking is applied to both wheelsets, skidding and instability happen to both wheelsets.
5. The computer program is capable of evaluation the resulting speed profile due to brake of application.
6. The computer program is also capable of evaluating skidding under heavy braking.

7. ACKNOWLEDGEMENT

This work reported in this paper is part of an ongoing research on the effect of brake force application to the wagon and bogie dynamics as well as wheel and railhead damages jointly funded by the CRE, CQU Australia and Indonesian Railways Industry (PT INKA).

REFERENCES

1. AEATechnologyRail, 'VAMPIRE, rail vehicle dynamics software,' http://www.vampire-dynamics.com2004.
2. Handoko, Y., Xia, F., and Dhanasekar, M., 'Effect of asymmetric brake shoe force application on wagon curving performance,' in Vehicle System Dynamic Supplement, vol. 41, pp. 113-122, 2004.
3. Macfarlane, I., 'Brakes,' in Railway safety, R. Hope, Ed., Engineer Australia Pty Limited2000.
4. Shabana, A. A., Berzerri, M., and Sany, J. R., 'Numerical procedure for the simulation of wheel/rail contact dynamics,' in Journal of Dynamic System, Measurement, and Control, vol. 123, pp. 168-178, 2001.
5. Eich-Sollner, E. and Fuhrer, C., 'Numerical method in multibody dynamics', B. G. Teubner,Stuttgart, 1998.
6. Sun, Y. Q. and Dhanasekar, M., 'Importance of track modeling to the determination of the critical speed of wagons,' in 18th IAVSD Symposium, Kanagawa, Japan, 2004.
7. Esveld, C., 'Modern railway track', MRT Production, Netherland, 2001.